

## $\gamma$ -Ray Flashes from Dark Photons in Neutron Star Mergers

Melissa D. Diamond<sup>1,\*</sup> and Gustavo Marques-Tavares<sup>2,†</sup><sup>1</sup>*Department of Physics and Astronomy, Johns Hopkins University, Baltimore, Maryland 21218, USA*<sup>2</sup>*Maryland Center for Fundamental Physics, Department of Physics, University of Maryland, College Park, Maryland 20742, USA* (Received 6 July 2021; revised 3 March 2022; accepted 14 April 2022; published 24 May 2022)

In this Letter we begin the study of visible dark sector signals coming from binary neutron star mergers. We focus on dark photons emitted in the 10 ms–1 s after the merger, and show how they can lead to bright transient  $\gamma$ -ray signals. The signal will be approximately isotropic, and for much of the interesting parameter space will be close to thermal, with an apparent temperature of  $\sim 100$  keV. These features can distinguish the dark photon signal from the expected short  $\gamma$ -ray bursts produced in neutron star mergers, which are beamed in a small angle and nonthermal. We calculate the expected signal strength and show that for dark photon masses in the 1–100 MeV range it can easily lead to total luminosities larger than  $10^{46}$  ergs for much of the unconstrained parameter space. This signal can be used to probe a large fraction of the unconstrained parameter space motivated by freeze-in dark matter scenarios with interactions mediated by a dark photon in that mass range. We also comment on future improvements when proposed telescopes and midband gravitational detectors become operational.

DOI: [10.1103/PhysRevLett.128.211101](https://doi.org/10.1103/PhysRevLett.128.211101)

*Introduction.*—The detection of gravitational waves (GW) from binary neutron star (BNS) mergers, and the observation of their electromagnetic counterparts has inaugurated a new era in multimessenger astronomy [1–3]. Upcoming observations will shed light on the physics of neutron stars, the origin of heavy elements, and models of stellar evolution [4–7]. This new window into the Universe offers great potential as a probe of physics beyond the standard model (SM), and in particular of scenarios involving very weakly interacting new states.

When two neutron stars merge, a metastable remnant with nuclear densities and temperatures in the 10 s of MeV forms, similar to the proton-neutron stars formed in core-collapse supernovae [8–11]. These hot remnants are a promising source of new weakly coupled particles. It has already been shown that such events can produce a large flux of neutrinos [12]. Nonetheless, the low merger rate implies that if we are interested in seeing at least  $\mathcal{O}(1)$  merger per year, their typical distance will be  $\sim 100$  Mpc, making direct observation of the new particles challenging due to their small flux at large distances and small couplings. However, if the new particles are unstable and can decay to visible particles, such as leptons or photons, they can produce very bright signals making BNS mergers a powerful probe of new physics.

There have been a number of proposals to search for new physics affecting the GW signal from binary black holes or neutron star mergers [13–20], in addition to potential cooling constraints due to the emission of weakly coupled BSM particles from the remnant [21,22]. In this Letter, we initiate the study of dark sector electromagnetic signals in BNS mergers. For concreteness, we focus exclusively on dark photons, though this framework is applicable to other dark sector models. The dark photon is a new massive vector field that kinetically mixes with the photon, and through this mixing interacts with charged standard model matter [23,24]. It corresponds to one of the three renormalizable portals between the standard model (SM) and dark sectors, which are sectors not charged under the SM gauge group [25,26]. Dark matter might be part of such a dark sector, and its interactions with the standard model mediated by the dark photon may account for the observed dark matter density. The relic abundance can be obtained either through standard freeze-out, corresponding to scenarios in which dark matter reaches thermal equilibrium with the visible sector and requires larger couplings, or through freeze-in in which the interactions are so weak that dark matter never reaches thermal equilibrium with the SM [27,28].

The cross sections suggested by the freeze-out scenario motivated a large experimental program intended to cover the parameter space corresponding to the observed relic density. In contrast, the freeze-in scenario points to tiny couplings, with the kinetic mixing parameter as small as  $10^{-11}$ , making it more difficult to probe experimentally. There are a number of recent direct detection proposals

---

*Published by the American Physical Society under the terms of the Creative Commons Attribution 4.0 International license. Further distribution of this work must maintain attribution to the author(s) and the published article's title, journal citation, and DOI. Funded by SCOAP<sup>3</sup>.*

aimed at probing the freeze-in parameters for very light dark photons, which take advantage of the cross section enhancement at low velocities characteristic of interactions mediated by light particles (e.g., Refs. [29–32]). Probing the freeze-in scenario for larger dark photon masses, when there is no significant enhancement of the cross section, is much more challenging. Most constraints on this scenario come from searches sensitive to the dark photon directly, generally using cosmological or astrophysical signals [33–40]. We will show that dark photons in the mass range  $\sim 1$ –100 MeV can be produced copiously in the remnant of a neutron star merger. Their decays lead to a transient bright  $\gamma$ -ray signal that can be used to search for dark photons in much of the remaining viable parameter space for freeze-in with a mediator in that mass range.

*Dark photon production and decay.*—We will concentrate on dark photon production and assume that any other new particles are heavy and irrelevant for BNS mergers. The relevant terms in the Lagrangian are

$$\mathcal{L} \supset \frac{1}{2} m' A'_\mu A'^\mu - \frac{1}{4} F'_{\mu\nu} F'^{\mu\nu} - \frac{\epsilon}{2} F'_{\mu\nu} F^{\mu\nu}, \quad (1)$$

where  $A'^\mu$  is the dark photon,  $m'$  its mass,  $F^{\mu\nu}$  the photon field strength, and  $\epsilon$  the kinetic mixing.

The production of dark photons in the protoneutron star is dominated by nucleon-nucleon bremsstrahlung, as in the supernova case. The flux of dark photons can be calculated following Ref. [37],

$$\frac{dN}{dV dt} = \int \frac{d\omega \omega^2 v}{2\pi^2} e^{-\omega/T} (\Gamma_{\text{abs},L} + 2\Gamma_{\text{abs},T}), \quad (2)$$

where  $\omega$  is the frequency of the dark photon,  $v$  its velocity,  $T$  the local temperature, and  $\Gamma_{\text{abs},T(L)}$  the absorption width for the transverse (longitudinal) dark photon modes. Integrating this over the production volume gives the total number of dark photons produced. The absorption width can be computed using the soft-radiation approximation, as discussed in Ref. [41]. Ignoring Pauli blocking [which is at most an  $\mathcal{O}(1)$  effect], we find

$$\Gamma_{\text{abs},X} = \frac{32\alpha n_n n_p \epsilon^2 m'^4}{3\pi\omega^3 [(m'^2 - \text{Re}\Pi_X)^2 + \text{Im}\Pi_X^2]} \left(\frac{\pi T}{m_N}\right)^{3/2} \times \langle \sigma_{\text{np}}^{(2)}(T) \rangle \times \begin{cases} 1, & X = T \\ (m'/\omega)^2, & X = L \end{cases}, \quad (3)$$

where  $X = T(L)$  refers to the transverse (longitudinal) polarization of the dark photon,  $m_N$  is the nucleon mass,  $n_{n(p)}$  is the neutron (proton) density,  $\Pi_X$  is the in medium polarization tensor of the photon (see Supplemental Material [42] for their explicit form), and  $\langle \sigma_{\text{np}}^{(2)} \rangle$  is the weighted proton neutron scattering cross section taken from Ref. [41]. From Eq. (2), we calculate the dark photon luminosity

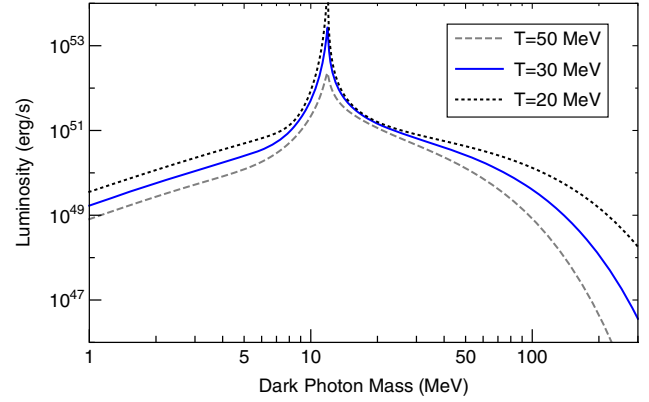


FIG. 1. Luminosity of dark photons with  $\epsilon = 10^{-10}$ , produced in BNS mergers using the simplified profile. We use  $T = 30$  MeV (blue curve) for calculations in this Letter. The dashed and dotted lines show luminosity for other values of temperature. The enhancement near 10 MeV comes from resonant mixing between the dark photon and the photon.

$$\frac{dE}{dV dt} = \int \frac{d\omega \omega^3 v}{2\pi^2} e^{-\omega/T} (\Gamma_{\text{abs},L} + 2\Gamma_{\text{abs},T}). \quad (4)$$

Based on BNS merger simulations in Refs. [9–11,45], we assume a simplified, spherically symmetric description of the merger remnant, with a constant temperature, density, and electron fraction:  $T = 30$  MeV,  $\rho = 4 \times 10^{14}$  g cm $^{-3}$ , and  $Y_e = 0.1$  in the region 5–10 km from the center of the remnant. We consider only the dark photons produced in this hot region and ignore contributions from other colder regions. In Fig. 1, we show the luminosity of dark photons as a function of mass and how it varies with the remnant’s temperature.

The time evolution of the remnant depends on the mass of the original neutron stars and the equation of state of nuclear matter. Different initial conditions can produce a variety of different remnants that persist for 1–1000 ms before collapsing to a black hole [8–11,45]. Light remnants might not collapse at all, instead forming a heavier neutron star [46]. Nonetheless, cooling will decrease their temperature from  $T \sim 30$  MeV within a few seconds [21,47]. To illustrate this range of possibilities, we present results assuming two different scenarios for dark photon emissions: emissions lasting 10 ms after the merger and emissions lasting 1 s after the merger. Note that most analyses of GW170817 conclude that the remnant must have lasted for at least 10 ms [48–51]. For simplicity, we ignore gravitational redshift, which depends strongly on the density distribution in the central region of the merger (we estimate its impact in the Supplemental Material [42]).

After production, the dark photons decay to electron-positron pairs, forming an expanding plasma shell. The dark photon decay width at rest is

$$\Gamma = \frac{1}{3} \alpha \epsilon^2 m' \sqrt{1 - \frac{4m_e^2}{m'^2} \left(1 + \frac{2m_e^2}{m'^2}\right)}, \quad (5)$$

where  $m_e$  is the electron mass. The initial Lorentz factor of the expanding shell is approximately the average Lorentz factor of the dark photon flux,

$$\gamma_0 = \frac{\langle \omega \rangle}{m'}, \quad (6)$$

where  $\langle \omega \rangle$  is the average dark photon energy. In the merger frame, the dark photon decay length is

$$d = \frac{\gamma_0 v}{\Gamma}. \quad (7)$$

The width of the plasma shell immediately after the decay is

$$\delta = \frac{1}{\gamma_0 \Gamma}, \quad \delta' = \frac{1}{\Gamma} \quad (8)$$

in the star frame and plasma frame respectively.

The photon signal depends on the evolution of this plasma. For simplicity, we focus on parameters such that the dark photons decay least 1000 km from the center of the merger, where ambient baryon density and magnetic fields can be safely neglected. (Magnetic fields do not directly affect the dark photons, but would lead to nontrivial dynamics for the electron-positron plasma formed after the decay.) When calculating the number of leptons that results from dark photon decays, we only include the fraction coming from decays at least 1000 km away from the merger. Dark photons in most of the viable parameter space have long enough decay lengths that this requirement does not cause a significant change in sensitivity.

*$\gamma$ -ray signal.*—We are interested in the photon signal arising from the electrons and positrons produced by dark photon decays. With our simplified approximation for the remnant, the signal will be isotropic (Realistic remnants will not be spherically symmetric, but for observers at large distances the signal would still be isotropic.), peaked between 100 keV and 10 s of MeV, and visible within about a second of the merger. The isotropic nature of the signal, its duration, and its spectral information can be used to distinguish it from the short  $\gamma$ -ray burst expected to be produced from relativistic jets after the remnant collapses to a black hole [3,52].

We track the dynamics of the plasma starting from a radius equal to the decay length of the dark photon in the star frame, given by Eq. (7). We describe the plasma using quantities defined in the coexpanding frame, in which the lepton momenta distribution is isotropic and which is initially related to the merger frame by a Lorentz factor given by Eq. (6). In this frame, the initial temperature is directly related to the dark photon mass,  $T \approx m'/6$ , since in

that frame each electron and positron generated by the dark photon has approximately  $m'/2$  energy, with a small spread related to the dark photon boost distribution. The initial number density is given by

$$n_e \approx \frac{N_{\text{tot}} \gamma_0}{4\pi d^3}, \quad (9)$$

where we take

$$N_{\text{tot}} = \frac{dN}{dV dt} \times V_{\text{emit}} t_{\text{emit}} (e^{-1000 \text{ km}/d} - e^{-1}) \quad (10)$$

as the number of dark photons which decay between 1000 km and one decay length from the merger remnant.  $V_{\text{emit}}$  and  $t_{\text{emit}}$  are the volume and time over which dark photons are emitted, respectively. As in the standard fireball model [52,53], when the plasma energy is dominated by relativistic particles, the density evolves as  $\rho \propto r^{-4}$ , where  $r$  is the distance of the plasma shell from the remnant (in the remnant's rest frame), the Lorentz factor of the shell increases as  $\gamma \propto r$ , and the width in the merger frame, which also determines the duration of the signal, remains constant. If expansion is the only process which changes the total number density then the total number of particles is conserved, the total number density scales as  $n \propto r^{-3}$ , and the temperature goes as  $T \propto r^{-1}$ .

The electron-positron densities in the plasma can be large enough for pair annihilation,  $e^+ e^- \rightarrow \gamma\gamma$ , to be very efficient. In this case, the pair creation and annihilation processes quickly lead the number densities of electrons and photons to be related by detailed balance,

$$\frac{n_e}{n_\gamma} = \frac{n_e^{\text{eq}}}{n_\gamma^{\text{eq}}}. \quad (11)$$

The rhs of Eq. (11) refers to the equilibrium number densities for leptons and photons. In this regime, the photon mean free path will be short, and the plasma is optically thick. An observable signal emerges once the lepton number density becomes low enough for the plasma to become optically thin, allowing photons to escape. Photon bremsstrahlung from electron and positron scattering can also play an important role in the dynamics of the plasma. While pair creation or annihilation preserves the total number of particles, bremsstrahlung increases the total number of particles and consequently the total number density. Energy conservation implies that the temperature decreases as the number density goes up; thus, bremsstrahlung can lower the peak energy of the photon signal.

To determine if pair annihilation and bremsstrahlung are important effects, we compare their rates in the plasma frame to the number density dilution rate coming from the expansion,

$$\Gamma_{\text{exp}} = -3\gamma/r. \quad (12)$$

The rate for pair annihilation is given by [54]

$$\Gamma_{\text{annih}} \approx \frac{\pi n_e \alpha^2}{m_e^2} \left( 1 + \frac{2(T/m_e)^2}{1 + \log\left(\frac{2T}{m_e e^{\gamma_E}} + 1.3\right)} \right)^{-1}, \quad (13)$$

where  $\gamma_E$  is the Euler-Mascheroni constant. The photon production rate from  $e^+e^-$  (or  $e^-e^-$ ) bremsstrahlung in a relativistic gas ( $T \gg m_e^2$ ) is [55]

$$\Gamma_{\text{brem}} \approx \frac{2n_e \alpha^3 \log(e^{\gamma_E} m_e^2/T^2)}{9m_e^2} [12 \log(e^{\gamma_E} m_e^2/T^2) - 84 + 48 \log(e^{\gamma_E} m_e/T)], \quad (14)$$

where we imposed an infrared cutoff on the photon energy  $\omega_\gamma > m_e^2/T$ , corresponding to photons that can exchange  $\mathcal{O}(T)$  of energy in a single scattering and thus quickly thermalize. For  $T \lesssim 1$  MeV, we switch to the nonrelativistic rate (for the dominant  $e^+e^-$  case) [56]

$$\Gamma_{\text{brem}} \approx \frac{64}{3\sqrt{\pi}} \frac{n_e \alpha^3}{\sqrt{T} m_e^3}, \quad (15)$$

where we imposed an infrared cutoff  $\omega_\gamma > T$ , again corresponding to photons that can exchange  $\mathcal{O}(T)$  energy in a single scattering. If the annihilation and bremsstrahlung rates are both greater than the expansion rate at the beginning of the plasma evolution, right after most dark photons have decayed, then the plasma thermalizes quickly. Since  $n_\gamma \ll T^3$ , these processes increase the total number

density and decrease the temperature before any significant expansion until  $T \leq m_e$ , at which point both annihilation and bremsstrahlung rates decay exponentially due to the loss of leptons. Dark photons with masses above  $\sim 10$  MeV have another mechanism for thermalizing rapidly. Even if the pair annihilation rate is initially slower than the expansion, the energy loss rate from bremsstrahlung [55]

$$\left. \frac{d \log \rho_e}{dt} \right|_{\text{brem}} = -\frac{8n_e \alpha^3}{m_e^2} \left[ \text{Log} \left( \frac{2T}{e^{\gamma_E} m_e} \right) + \frac{5}{4} \right] \quad (16)$$

can be faster than that due to expansion

$$\left. \frac{d \log \rho_e}{dt} \right|_{\text{exp}} = -\frac{4\gamma}{r}, \quad (17)$$

where  $\rho_e = 3Tn_e$  is the energy density of the shell in the shell frame immediately after the dark photons' decay. This energy loss decreases the plasma temperature (with insignificant change to the lepton number density), increasing the pair annihilation rate sufficiently to make it faster than the expansion. Afterward, the fireball evolves as if both pair annihilation and bremsstrahlung were already efficient when the plasma first formed.

The resulting photon spectrum in the observer frame is approximately thermal, with an apparent temperature given by  $\gamma_* T_*$ , where  $\gamma_*$  and  $T_*$  are respectively the plasma's Lorentz factor and temperature when it becomes optically thin for photons. The photon interaction rate drops exponentially once the plasma temperature is below  $m_e$  because the electron density becomes Boltzmann suppressed, leading to  $T_* \sim m_e/10$  with only a mild logarithmic sensitivity to the initial conditions of the plasma shell. In the

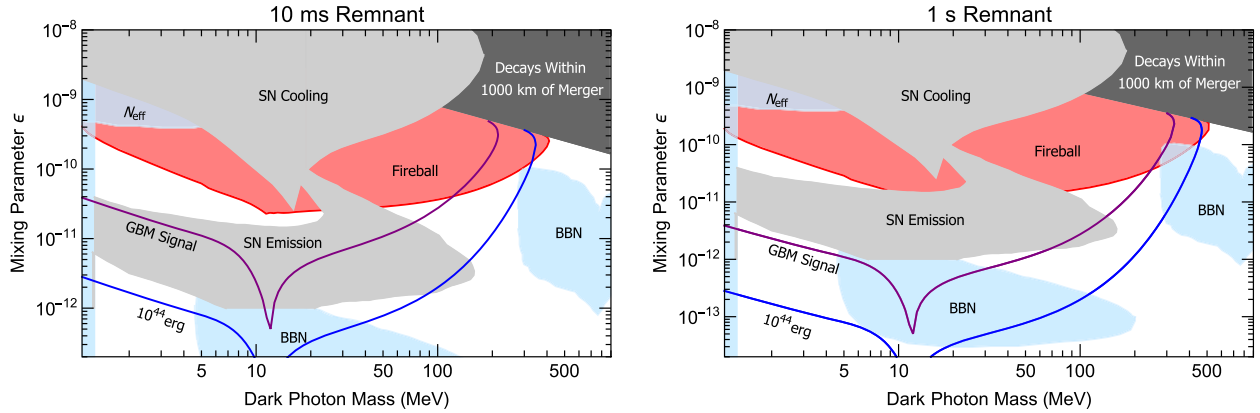


FIG. 2. The left (right) plot shows the conditions produced when the merger emits dark photons for 10 ms (1 s). The red region marks where the dark photons form a fireball which produces a thermal spectrum; below it dark photons generate a dimmer nonthermal signal. The dark gray region shows where the dark photon decay length is less than 1000 km (close enough to the merger remnant that baryons could affect the signal). The purple line shows the minimum  $\epsilon$  needed to produce a signal visible to Fermi GBM for a merger 100 Mpc away ( $\sim 2 \times 10^{46}$  ergs), and the blue line shows parameters for a  $10^{44}$  erg signal. The light gray regions marked SN Cooling and SN Emission show the parameter space already ruled out by astrophysical observations [37,39]. The light blue regions labeled  $N_{\text{eff}}$  and BBN mark space excluded by cosmological observations [35,57–59]. For potential additional complementary constraints, see also Refs. [39,60,61].

thermalized scenario, the temperature drops before the plasma expands significantly, and thus  $\gamma_* = \gamma_0 \lesssim 10$ , and effectively all of the energy radiated in dark photons gets converted into photons with energies in the 10–1000 keV range. The photon signal duration is set by a light crossing time of the plasma shell, about 0.1–100 s depending on the dark photon parameters. The luminosity of the signal can be estimated by dividing the total energy output by the width of the plasma shell as shown in Eq. (8).

The parameter space region in which this thermal spectrum occurs is shown in Fig. 2 for two different assumptions about the duration of the remnant. It also shows two curves which mark the total energy emitted in dark photons. One curve shows where the signal would be detectable at the Fermi  $\gamma$ -ray burst monitor (GBM), assuming all of the energy gets converted to photons in the sensitivity range of the instrument (100–2000 keV) and a merger distance of 100 Mpc. The other curve shows the region where the total energy emitted in dark photons is  $10^{44}$  ergs as a potential target for future detectors. If the “fireball” forms, the dark photon energy would get converted to the GBM range because the initial boost  $\gamma_0$  is  $\mathcal{O}(1)$  for all relevant masses. This shows that one could probe most of the remaining parameter space above  $\epsilon \approx 10^{-11}$ , motivated by freeze-in dark matter scenarios, for  $m' \approx 1$ –100 MeV by searching for  $\gamma$ -ray signals which coincide with a neutron star merger.

*Discussion and future prospects.*—The LIGO/Virgo collaboration is currently sensitive to neutron star mergers within  $\sim 100$  Mpc of Earth [62]. The first BNS merger detection, GW170817, was about half this distance, unusually close given the estimated rate for BNS mergers. There was an associated  $\gamma$ -ray signal observed shortly after by Fermi-GBM and Integral [63], which has largely confirmed the expectation that BNS mergers are responsible for short  $\gamma$ -ray bursts (SGRB). Making a discovery of dark photons using the  $\gamma$ -ray signal discussed in this Letter would require distinguishing the dark photon signal from usual SGRBs. This can, in principle, be done using the fact that SGRBs are expected to be highly beamed since they are produced by a relativistic jet, leading to large variations of the observed luminosity from mergers at similar distances. However, potential off-axis  $\gamma$ -ray emission is still not fully understood, and might be an important background for our proposal [64–66]. Even if there is a significant background from off-axis emission, one can use information about the spectrum, signal arrival time, and duration as important features to distinguish our signal from SGRBs (in the Supplemental Material [42] we show how timing can be used to put constraints on the dark photon model).

The LIGO/Virgo collaboration will be sensitive to neutron star mergers as far as  $\sim 200$  Mpc when it reaches design sensitivity in the near future [67], at which point it will detect multiple mergers per year. Having large merger statistics, and utilizing realistic remnant profiles from

simulations, would allow one to probe the parameter space in Fig. 2 above the purple line and within the fireball region assuming better understanding of the backgrounds from SGRBs. This would cover a large portion of the remaining parameter space motivated by dark matter freeze-in,  $\epsilon \gtrsim 10^{-11}$  [28].

There are two challenges to probing the parameter space in which a fireball never forms. One is modeling the multiple processes that produce photons from a dilute electron-positron plasma. We leave the required detailed analysis of this nonthermal emission to future work, but we expect that for part of the parameter space, the main signal will be in  $\sim 10$  MeV photons, for which we currently do not have very good coverage. There are a number of proposals such as e-ASTROGRAM [68], AMEGO [69], and MeVCube [70] that target the low MeV range which would significantly increase our reach to dark photons from BNS. The other challenge is that, for smaller couplings, the lepton density after decay is smaller, and only a reduced fraction of the energy gets converted to photons, making the signal dimmer. One promising direction to compensate for the low photon luminosity is to use detectors with better angular resolution, which decreases the background to the signal. Future proposed GW mid-band detectors such as AMIGO [71], MAGIS [72], AION [73], and ELGAR [74] should be able to detect BNS merger events in advance and with better localization, allowing future x-ray and  $\gamma$ -ray telescopes with narrower fields of view to observe the merger.

We have shown that neutron star mergers can be used to search for unstable dark sector particles. We demonstrated this by studying the  $\gamma$ -ray signatures that arise from dark photon decays, and showed that this can probe a large portion of unconstrained parameter space, including much of the remaining parameter space motivated by dark matter freeze-in. Utilizing the full potential of BNS as probes of dark sectors requires a better understanding of the remnant dynamics and further investigation of how to distinguish the signal arising from dark sectors from that expected from SGRBs associated with BNS mergers.

The authors thank Tim Dietrich, Julian Krolik, and David Radice for useful discussions and Daniel Egaña-Ugrinovic for comments on the draft. G. M. T. was supported in part by the NSF Grants No. PHY-1914480 and No. PHY-1914731, by the Maryland Center for Fundamental Physics (MCFP), and by the US-Israeli BSF Grant No. 2018236. M. D. was supported in part by NSF Grant No. PHY-1818899.

\*mdiamon8@jhu.edu

†gusmt@umd.edu

[1] B. P. Abbott *et al.* (LIGO Scientific, Virgo Collaborations), *Phys. Rev. Lett.* **119**, 161101 (2017).

- [2] B. P. Abbott *et al.* (LIGO Scientific, Virgo, Fermi GBM, INTEGRAL, IceCube, AstroSat Cadmium Zinc Telluride Imager Team, IPN, Insight-Hxmt, ANTARES, Swift, AGILE Team, 1M2H Team, Dark Energy Camera GWEM, DES, DLT40, GRAWITA, Fermi-LAT, ATCA, ASKAP, Las Cumbres Observatory Group, OzGrav, DWF (Deeper Wider Faster Program), AST3, CAASTRO, VINROUGE, MASTER, J-GEM, GROWTH, JAGWAR, CaltechNRAO, TTU-NRAO, NuSTAR, Pan-STARRS, MAXI Team, TZAC Consortium, KU, Nordic Optical Telescope, ePESSTO, GROND, Texas Tech University, SALT Group, TOROS, BOOTES, MWA, CALET, IKI-GW Follow-up, H.E.S.S., LOFAR, LWA, HAWC, Pierre Auger, ALMA, Euro VLBI Team, Pi of Sky, Chandra Team at McGill University, DFN, ATLAS Telescopes, High Time Resolution Universe Survey, RIMAS, RATIR, SKA South Africa/MeerKAT Collaborations), *Astrophys. J. Lett.* **848**, L12 (2017).
- [3] B. P. Abbott *et al.* (LIGO Scientific, Virgo, Fermi-GBM, INTEGRAL Collaborations), *Astrophys. J. Lett.* **848**, L13 (2017).
- [4] J. J. Cowan, C. Sneden, J. E. Lawler, A. Aprahamian, M. Wiescher, K. Langanke, G. Martínez-Pinedo, and F.-K. Thielemann, *Rev. Mod. Phys.* **93**, 015002 (2021).
- [5] P. Meszaros, *Annu. Rev. Astron. Astrophys.* **40**, 137 (2002).
- [6] E. Pian, *Front. Astron. Space Sci.* **7**, 108 (2021).
- [7] P. Mészáros, D. B. Fox, C. Hanna, and K. Murase, *Nat. Rev. Phys.* **1**, 585 (2019).
- [8] G. Camelio, T. Dietrich, S. Rosswog, and B. Haskell, *Phys. Rev. D* **103**, 063014 (2021).
- [9] A. Endrizzi, A. Perego, F. M. Fabbri, L. Branca, D. Radice, S. Bernuzzi, B. Giacomazzo, F. Pederiva, and A. Lovato, *Eur. Phys. J. A* **56**, 15 (2020).
- [10] D. Radice, *Symmetry* **12**, 1249 (2020).
- [11] A. Perego, S. Bernuzzi, and D. Radice, *Eur. Phys. J. A* **55**, 124 (2019).
- [12] D. Radice, A. Perego, K. Hotokezaka, S. A. Fromm, S. Bernuzzi, and L. F. Roberts, *Astrophys. J.* **869**, 130 (2018).
- [13] S. Endlich, V. Gorbenko, J. Huang, and L. Senatore, *J. High Energy Phys.* **09** (2017) 122.
- [14] A. Hook and J. Huang, *J. High Energy Phys.* **06** (2018) 036.
- [15] L. Sagunski, J. Zhang, M. C. Johnson, L. Lehner, M. Sakellariadou, S. L. Liebling, C. Palenzuela, and D. Neilsen, *Phys. Rev. D* **97**, 064016 (2018).
- [16] D. Croon, A. E. Nelson, C. Sun, D. G. E. Walker, and Z.-Z. Xianyu, *Astrophys. J. Lett.* **858**, L2 (2018).
- [17] J. Huang, M. C. Johnson, L. Sagunski, M. Sakellariadou, and J. Zhang, *Phys. Rev. D* **99**, 063013 (2019).
- [18] M. Bezares, D. Viganò, and C. Palenzuela, *Phys. Rev. D* **100**, 044049 (2019).
- [19] J. A. Dror, R. Laha, and T. Opferkuch, *Phys. Rev. D* **102**, 023005 (2020).
- [20] N. Sennett, R. Brito, A. Buonanno, V. Gorbenko, and L. Senatore, *Phys. Rev. D* **102**, 044056 (2020).
- [21] T. Dietrich and K. Clough, *Phys. Rev. D* **100**, 083005 (2019).
- [22] S. P. Harris, J.-F. Fortin, K. Sinha, and M. G. Alford, *J. Cosmol. Astropart. Phys.* **07** (2020) 023.
- [23] B. Holdom, *Phys. Lett.* **166B**, 196 (1986).
- [24] M. Fabbrichesi, E. Gabrielli, and G. Lanfranchi, *The Physics of the Dark Photon* (Springer, New York, 2021).
- [25] R. Essig *et al.*, in Community Summer Study 2013: Snowmass on the Mississippi (2013), [arXiv:1311.0029](https://arxiv.org/abs/1311.0029).
- [26] J. Alexander *et al.*, [arXiv:1608.08632](https://arxiv.org/abs/1608.08632).
- [27] L. J. Hall, K. Jedamzik, J. March-Russell, and S. M. West, *J. High Energy Phys.* **03** (2010) 080.
- [28] X. Chu, T. Hambye, and M. H. G. Tytgat, *J. Cosmol. Astropart. Phys.* **05** (2012) 034.
- [29] R. Essig, M. Fernandez-Serra, J. Mardon, A. Soto, T. Volansky, and T.-T. Yu, *J. High Energy Phys.* **05** (2016) 046.
- [30] S. Knapen, T. Lin, M. Pyle, and K. M. Zurek, *Phys. Lett. B* **785**, 386 (2018).
- [31] O. Abramoff, L. Barak, I. M. Bloch, L. Chaplinsky, M. Crisler *et al.* (SENSEI Collaboration), *Phys. Rev. Lett.* **122**, 161801 (2019).
- [32] T. Aralis *et al.* (SuperCDMS Collaboration), *Phys. Rev. D* **101**, 052008 (2020); **103**, 039901(E) (2021).
- [33] J. Redondo and M. Postma, *J. Cosmol. Astropart. Phys.* **02** (2009) 005.
- [34] H. An, M. Pospelov, and J. Pradler, *Phys. Lett. B* **725**, 190 (2013).
- [35] A. Fradette, M. Pospelov, J. Pradler, and A. Ritz, *Phys. Rev. D* **90**, 035022 (2014).
- [36] D. Kazanas, R. N. Mohapatra, S. Nussinov, V. L. Teplitz, and Y. Zhang, *Nucl. Phys.* **B890**, 17 (2014).
- [37] J. H. Chang, R. Essig, and S. D. McDermott, *J. High Energy Phys.* **01** (2017) 107.
- [38] E. Hardy and R. Lasenby, *J. High Energy Phys.* **02** (2017) 033.
- [39] W. DeRocco, P. W. Graham, D. Kasen, G. Marques-Tavares, and S. Rajendran, *J. High Energy Phys.* **02** (2019) 171.
- [40] D. K. Hong, C. S. Shin, and S. Yun, *Phys. Rev. D* **103**, 123031 (2021).
- [41] E. Rrapaj and S. Reddy, *Phys. Rev. C* **94**, 045805 (2016).
- [42] See Supplemental Material at <http://link.aps.org/supplemental/10.1103/PhysRevLett.128.211101>, which include references [43,44].
- [43] A. Hajela *et al.*, *Astrophys. J. Lett.* **886**, L17 (2019).
- [44] B. Margalit and B. D. Metzger, *Astrophys. J. Lett.* **850**, L19 (2017).
- [45] S. Bernuzzi *et al.*, *Mon. Not. R. Astron. Soc.* **497**, 1488 (2020).
- [46] S. Fujibayashi, S. Wanajo, K. Kiuchi, K. Kyutoku, Y. Sekiguchi, and M. Shibata, *Astrophys. J.* **901**, 122 (2020).
- [47] D. Radice, S. Bernuzzi, and A. Perego, *Annu. Rev. Nucl. Part. Sci.* **70**, 95 (2020).
- [48] A. Murguia-Berthier, E. Ramirez-Ruiz, F. De Colle, A. Janiuk, S. Rosswog, and W. H. Lee, *Astrophys. J.* **908**, 152 (2021).
- [49] M. Shibata, E. Zhou, K. Kiuchi, and S. Fujibayashi, *Phys. Rev. D* **100**, 023015 (2019).
- [50] M. Shibata, S. Fujibayashi, K. Hotokezaka, K. Kiuchi, K. Kyutoku, Y. Sekiguchi, and M. Tanaka, *Phys. Rev. D* **96**, 123012 (2017).
- [51] M. Ruiz, S. L. Shapiro, and A. Tsokaros, *Phys. Rev. D* **97**, 021501(R) (2018).
- [52] P. Meszaros, *Rep. Prog. Phys.* **69**, 2259 (2006).
- [53] T. Piran, *Phys. Rep.* **314**, 575 (1999).
- [54] R. Svensson, *Astrophys. J.* **258**, 321 (1982).

- [55] M. Alexanian, *Phys. Rev.* **165**, 253 (1968).
- [56] E. Haug, *Astron. Astrophys.* **148**, 386 (1985).
- [57] J. R. Ellis, G. B. Gelmini, J. L. Lopez, D. V. Nanopoulos, and S. Sarkar, *Nucl. Phys.* **B373**, 399 (1992).
- [58] L. Zhang, X. Chen, M. Kamionkowski, Z.-g. Si, and Z. Zheng, *Phys. Rev. D* **76**, 061301(R) (2007).
- [59] M. Ibe, S. Kobayashi, Y. Nakayama, and S. Shirai, *J. High Energy Phys.* **04** (2020) 009.
- [60] A. Sung, H. Tu, and M.-R. Wu, *Phys. Rev. D* **99**, 121305(R) (2019).
- [61] A. Caputo, H.-T. Janka, G. Raffelt, and E. Vitagliano, [arXiv:2201.09890](https://arxiv.org/abs/2201.09890).
- [62] A. Buikema, C. Cahillane, G. L. Mansell, C. D. Blair, R. Abbott, C. Adams, R. X. Adhikari, A. Ananyeva *et al.* (LIGO Instrument Science List), *Phys. Rev. D* **102**, 062003 (2020).
- [63] A. Goldstein *et al.*, *Astrophys. J. Lett.* **848**, L14 (2017).
- [64] D. Lazzati, A. Deich, B. J. Morsony, and J. C. Workman, *Mon. Not. R. Astron. Soc.* **471**, 1652 (2017).
- [65] O. Gottlieb, E. Nakar, T. Piran, and K. Hotokezaka, *Mon. Not. R. Astron. Soc.* **479**, 588 (2018).
- [66] D. Lazzati, *Front. Astron. Space Sci.* **7**, 78 (2020).
- [67] J. Aasi *et al.* (LIGO Scientific Collaboration), *Classical Quantum Gravity* **32**, 074001 (2015).
- [68] A. De Angelis *et al.* (e-ASTROGAM Collaboration), *Exp. Astron.* **44**, 25 (2017).
- [69] R. Caputo *et al.* (AMEGO Collaboration), [arXiv:1907.07558](https://arxiv.org/abs/1907.07558).
- [70] G. Lucchetta, M. Ackermann, R. Bühler, and F. Zappon, in *Space Telescopes and Instrumentation 2020: Ultraviolet to Gamma Ray*, edited by J.-W. A. den Herder, S. Nikzad, and K. Nakazawa, International Society for Optics and Photonics (SPIE, 2020), Vol. 11444, pp. 834–843.
- [71] W.-T. Ni, G. Wang, and A.-M. Wu, *Int. J. Mod. Phys. D* **29**, 1940007 (2020).
- [72] M. Abe, P. Adamson, M. Borcean, D. Bortoletto, K. Bridges, S. P. Carman, S. Chattopadhyay, J. Coleman, N. M. Curfman, K. DeRose *et al.*, *Quantum Sci. Technol.* **6**, 044003 (2021).
- [73] L. Badurina *et al.*, *J. Cosmol. Astropart. Phys.* **05** (2020) 011.
- [74] B. Canuel *et al.*, *Classical Quantum Gravity* **37**, 225017 (2020).